Energy 127 (2017) 730–742

Contents lists available at ScienceDirect

Energy

journal homepage: www.elsevier.com/locate/energy

Measurement of power loss during electric vehicle charging and discharging

Elpiniki Apostolaki-Iosifidou [a, *], Paul Codani [b], Willett Kempton [a, c]

[a] Department of Electrical and Computer Engineering, University of Delaware, USA
[b] GeePs – Group of Electrical Engineering Paris, UMR CNRS 8507, CentraleSupelec, University Paris-Sud, Universite Paris-Saclay, Sorbonne Universites, UPMC Univ Paris 06, France
[c] College of Earth, Ocean, and Environment, University of Delaware, USA

ARTICLE INFO

Article history:
Received 4 August 2016
Received in revised form
1 March 2017
Accepted 4 March 2017
Available online 7 March 2017

Keywords:
Electric vehicles
Energy efficiency
Power losses
Grid-integrated vehicles
Vehicle-to-grid
Dispatch algorithm

ABSTRACT

When charging or discharging electric vehicles, power losses occur in the vehicle and the building systems supplying the vehicle. A new use case for electric vehicles, grid services, has recently begun commercial operation. Vehicles capable of such application, called Grid-Integrated Vehicles, may have use cases with charging and discharging summing up to much more energy transfer than the charging only use case, so measuring and reducing electrical losses is even more important. In this study, the authors experimentally measure and analyze the power losses of a Grid-Integrated Vehicle system, via detailed measurement of the building circuits, power feed components, and of sample electric vehicle components. Under the conditions studied, measured total one-way losses vary from 12% to 36%, so understanding loss factors is important to efficient design and use. Predominant losses occur in the power electronics used for AC-DC conversion. The electronics efficiency is lowest at low power transfer and low state-of-charge, and is lower during discharging than charging. Based on these findings, two engineering design approaches are proposed. First, optimal sizing of charging stations is analyzed. Second, a dispatch algorithm for grid services operating at highest efficiency is developed, showing 7.0% to 9.7% less losses than the simple equal dispatch algorithm.

1. Introduction

Plug-in electric vehicle (EV) sales have rapidly climbed because society's environmental and energy security concerns have resulted in policies to encourage or subsidize purchase of such vehicles. Nevertheless, today's high battery costs result in higher vehicle prices, slowing sales relative to their market potential. One way of reducing the cost of ownership is to provide grid services from EVs, thus providing a revenue stream from parked vehicles when not in use [1]. Indeed, EVs are able to provide multiple grid services, enabling substantially higher penetration of variable generation from renewable power sources. For example [2], models a combination of solar, offshore wind and onshore wind with storage selected to minimize overall cost; EVs are selected as the primary grid storage in all resulting least-cost optimizations.

The grid services proposed include voltage regulation, frequency regulation, reserves, and, since these services trade in paying markets, EVs with the right policies can participate and be remunerated. The impact of EVs on the electric grid when providing voltage regulation is shown in Ref. [3]. A detailed description of EV flexibility services including the voltage regulation from market perspective can be found in Ref. [4], and an actual demonstration project of EV frequency regulation is described in Ref. [5]. Other studies schedule EV services for maximum profit [6], calculate profitability of grid services to show realistic net revenue [7], and model a French EV fleet [8].

The University of Delaware (UD) GIV system has been implemented commercially by Nuvve. In operation, individual EVs are able to charge as well as discharge, which, under grid-relevant control, has value (and now run on qualifying markets in the PJM Interconnection territory of the US, in Denmark and the UK). These controllable charge- and discharge-rate EVs can operate in Grid-Integrated Vehicles (GIV) mode, controlled by and reporting to a central aggregator. The aggregator presents the EV fleet to a grid entity, for example a transmission system operator (TSO), as if it were a single power resource. First commercially operated by UD and eVgo (then NRG) in early 2013 [9], this system is now being commercialized by Nuvve in multiple districts.

* Corresponding author.
E-mail address: elpiniki@udel.edu (E. Apostolaki-Iosifidou).

http://dx.doi.org/10.1016/j.energy.2017.03.015

Nomenclature

Δt	Simulation sample time (s)
Ah	Amp hour. One Ah = 3600 Coulombs (C), because 1C = 1 A * 1 s (Ah)
C_{in}	Ampere-seconds charged over the N number of cycles (A·s)
C_{out}	Ampere-seconds discharged over the N number of cycles (A·s)
$E_{AC_{in}}$	Cumulative energy flowing from the EVSE to the PEU during an entire experiment (Wh)
$E_{AC_{out}}$	Cumulative energy flowing from the PEU to the EVSE during an entire experiment (Wh)
$E_{DC_{in}}$	Cumulative energy flowing from the PEU to the battery during an entire experiment (Wh)
$E_{DC_{out}}$	Cumulative energy flowing from the battery to the PEU during an entire experiment (Wh)
I_{AC}	Instantaneous current on the AC line (A)
I_{DC}	Instantaneous current on the DC bus (A)
l	Percentage power losses of the component under study (%)
N	Number of cycles during one experiment
N_{EV}	Number of EVs
P_i^k	Instantaneous power of vehicle k at time i (W)
P_{in}	Instantaneous power flowing in the component under study (W)
P_{out}	Instantaneous power flowing out of the component under study (W)
P_{req_i}	Power requested by PJM at time i (W)
SOC_i^k	Instantaneous State of Charge (SOC) of vehicle k at time i (%)
t_i	Starting time of the ith Coulomb cycle
t_{c_i}	Duration of the charging mode of a single ampere-hour neutral cycle (s)
t_{d_i}	Duration of the discharging mode of a single ampere-hour neutral cycle (s)
V_{AC}	Instantaneous voltage on the AC line (V)
V_{DC}	Instantaneous voltage on the DC bus (V)

An optimizing aggregator developed by UD allows for the needs of individual drivers, who may choose to unplug and travel at any time, while providing the grid with reliable power [10]. It does so by implementing dispatch algorithms, responsible for allocating grid requests across the vehicle fleet and for dispatching power flows of individual vehicles, while still considering EV conditions (e.g., state-of-charge (SOC), battery temperature), expected future trips, or any other relevant information [11]. Several other dispatch algorithms have been proposed in the literature. For instance, reference [12] presents unidirectional dispatch strategies for an EV fleet providing ancillary services. Reference [13] suggests a dispatch solution for two-way flow using a quadratic problem formulation. Reference [14] compares a centralized and a decentralized dispatch algorithm, and [15], proposes charging strategies to limit battery degradation.

Although these studies and algorithms take into account many variables and parameters in order to control an EV fleet, none of them takes into account the varying energy losses between the grid connection point and the EV battery – at best, a steady loss factor is considered, despite prior articles showing that losses vary with variables like battery state of charge [16], or current of charging and discharging [17]. The omission of efficiency variation under varying conditions may lead to higher electric losses and thus higher costs during operations. Losses are especially problematic for high-duty-cycle GIV functions using bidirectional flow.

This article makes two advances. First, power losses are extensively measured, from grid to the EV battery and back to the grid, under different conditions. These measurements are generalized by deriving functions to predict power losses. Second, the article quantitatively evaluates whether losses should be taken into account when controlling EV charging and discharging patterns – both in normal charging and under bidirectional dispatch algorithms for grid services. The provision of grid services will change the charging (and discharging) duty cycle, from present-day design that charges only to refill the battery for driving. In the long term, EV charger-discharger characteristics should be designed for grid services use cases, but for now, the article evaluates the benefit of dispatch algorithms designed to consider today's charger-discharger efficiency parameters.

For some types of valuable grid services, a storage unit is subject to frequent charging and discharging cycles. The increased throughput makes measurement of power loss important to achieve efficient operation. Round-trip power losses from the grid entry point to the storage battery are measured, through a series of experiments that put the system under charging and discharging cycles.

For this study two vehicles were measured in great detail for many components under many different operating conditions. The same extensive effort could have been invested, for example, into fewer measurements of many vehicles, fewer variations in conditions, or many repetitions of the same measurement to provide error bars. The approach taken here is insightful while acknowledging tradeoffs, for example, that variance in measurements are not quantified.

In order to explore the application of these results, two charging specifications or decisions that incorporate the experimental results are proposed: first for simple overnight charging and then for provision of grid services. In the latter use case, two dispatch algorithms are compared: one dispatching the power equally among the vehicles, without consideration of the power losses previously experimentally assessed, and a second dispatching the power among EVs strategically in order to minimize the power losses.

The outline of the paper is as follows. Section 2 is a description of the system from which the losses were measured, including the measuring devices. Section 3 presents the experimental procedure for the different parts of the system. Experimental results are described in section 4 and discussed in section 5. These results are used in section 6 to explore two strategies for charging and grid services. Conclusions are presented in 7.

2. System components

In this section, the whole system being measured for power losses is described. Also, the measuring devices used are briefly presented. The system boundaries are delimited by the EV battery on one side, and by the customer grid connection point on the other. More details about this system, part of the UD eV2G project, can be found in Ref. [18].

The system components consist of two parts: *building* and *EV components*. The *building* part includes components from the connector and cord of the charging station, also known as Electric Vehicle Supply Equipment (EVSE), to the grid connection point. The grid connection point is typically the commercial meter point, so losses anywhere from here to the battery and back are of practical

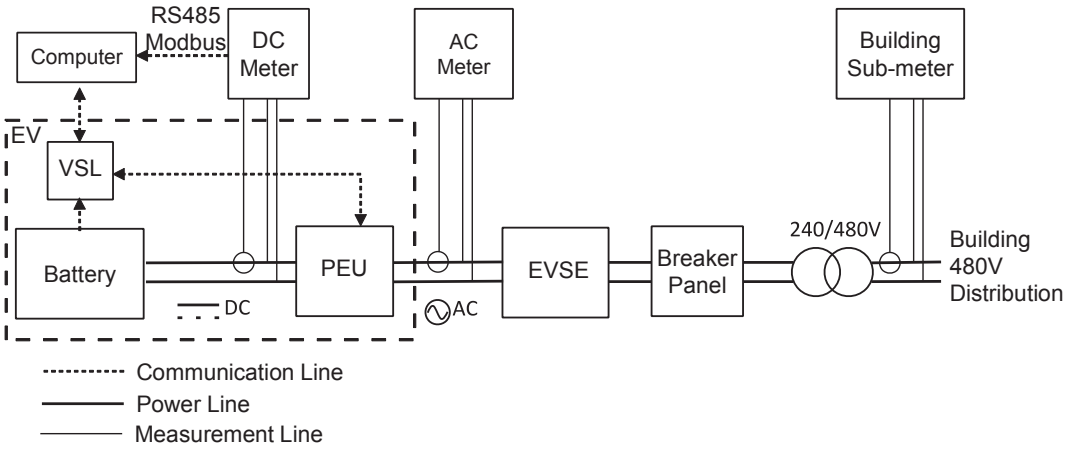

Fig. 1. System components overview. The AC meter is moved to other nodes, depending on the experiment.

revenue impact to the user or building owner. The *EV components* consist of the charger-discharger of the car, also known as the Power Electronics Unit (PEU), and the EV battery. The vehicle-side connector would technically be considered part of the car, but for measurement purposes is difficult to distinguish from the EVSE cord.

All the system components, the measuring devices, the power and the communication lines are shown in Fig. 1.

2.1. Building electrical components

The components making up the system without including the EV are:

Electric Vehicle Supply Equipment (EVSE): The EVSE, or charging station, is the interface between the EV and the building electrical system. Its primary function is to ensure a safe power connection between the EV and the grid by providing plug compatibility and security (e.g. a relay that closes on EV plug present, opens on ground fault). The EVSE is single phase with J1772 connector and CAN over control pilot communication.[1] Voltage at the charging station is 240 V from this circuit. Maximum current on the AC line is capped by vehicle limitation to 75 A, making maximum power flow 18 kW either charging or discharging. Like other AC EVSEs, the power circuit passes through only connectors, terminals and one relay, there are no active power electronics in the EVSE.[2]

Breaker Panel: Each EVSE is protected with a pair of 100 A circuit breakers, one on each conductor. All branch circuit breakers are within the panel, which is responsible for splitting the three-phase 240 V transformer output to the fifteen single-phase EVSEs. A main 900 A breaker protects the entire panel.

Transformer: The device furthest to the grid side analyzed here is a 300 kVA transformer that steps the 480 V building voltage down to the 240 V distribution panel. This might be called an intermediate transformer. The primary 12.47 kV transformer, from utility distribution to 480 V building power, is not considered here and is not shown in the diagram. In many US commercial buildings, the 480 V circuit would be the utility-metered circuit.

[1] CAN over control pilot is standardized in IEC 61851-1, Annex D, and is also being standardized in draft SAE J3068.

[2] DC EVSEs, not studied here, have essentially the same topology and efficiency consideration, but with the PEU moved out of the dotted boundary of the EV and placed inside the EVSE.

2.2. EV components

The experiments were conducted on two BMW MiniE vehicles. The University of Delaware, in collaboration with commercial partners BMW AG, AutoPort and NRG, has upgraded the vehicle to allow bi-directional power flow [9]. The electric vehicle can both charge the battery and also discharge power back to the grid. A fleet of these and other vehicles are aggregated and participate commercially in PJM's regulation market [5], and experimentally in other markets. A second MiniE was also measured but found to have atypically low PEU efficiency. Thus the second MiniE measurements are not averaged in but rather are cited occasionally when relevant to observations here.

The MiniEs have an access point to the DC battery bus right at the output of the battery pack. Connecting a DC meter to this bus enables the measurement of the EV battery voltage and current (DC values) in real time (see Appendix C for a description of the measuring devices). In order to control the car experimentally (set mode, current rate etc.), a UD-developed embedded controller and communications module is used. This module enables an EV to provide grid services, and is referred to as the Vehicle Smart Link (VSL). The VSL enables the communication with the car, (via a direct plug-in serial communication) and the control of the AC current rate and direction of both charging and discharging. Moreover, the VSL monitors and provides access to EV conditions, such as the battery SOC and temperature. Inside the EV, two vehicle components and one added control component are considered, shown in Fig. 1:

EV Battery: The battery pack purchased by AC Propulsion is composed of 48 $LiPF_6$ cobalt modules in series, providing a rated voltage of 345 V and a rated capacity of 106 Ah. Thus, the C-rate of the battery amounts to 106 A.

Power Electronics Unit (PEU): A power electronics system for converting from AC line voltage to the DC battery voltage and vice-versa, including cooling fans and other parasitic loads. In this study, the PEU is the AC-150 model made by AC Propulsion as a supplier to BMW.

Vehicle Smart Link (VSL): A small control module designed by UD and composed of EV-specific control circuits, plus an embedded UNIX machine. It manages communication with the EVSE and the EV's CANBus, stores user plans for trips, manages charging, and acts as an "EV Agent" in response to the optimizing aggregator. These characteristics make the EV capable of providing value to the power grid [11]. For these experiments,

the VSL is a convenient way to directly control rate and direction of power flow into and out of the vehicle.

2.3. Measuring devices

The measuring devices used for the experiments are:

AC Meter: The DM-II PLUS Power Quality Analyzer manufactured by Amprobe company was used for the AC measurements [19]. Additionally, in the EVSE an AC meter is installed named EKM Omnimeter Pulse v.4 [20]. This meter is permanently located between the PEU and the EVSE, as shown in Fig. 1. The DM-II PLUS device, when testing the building electrical components, has been used in various locations depending on the component under test. This device along with a hall effect sensor measures and records the AC current and voltage, as well as the active and reactive power. The accuracy of the devices is presented in Table 1 and the calibration information in Appendix C.

DC Meter: The AcuDC 243-C DC meter manufactured by AccuEnergy company was used to measure DC values on the DC battery bus [21]. This device measures and records DC current, voltage and power. This meter is also able to communicate in real-time via RS485 Modbus serial communication. A hall effect sensor was required to measure the battery current and provide the AcuDC 243-C meter with a voltage signal proportional to the current value. The CYHCS-WLY-300A-14 hall effect sensor from ChenYang Technologies company was used [22]. The accuracy of the devices is presented in Table 1 and the calibration information in Appendix C.

Building Sub-meter: The building sub-meter made by ION, measuring the 480 V side of the 240/480 V transformer, is permanently installed for this project, in order to continuously record the summed in-and-out energy for the GIV operation in this building. It was used only for the transformer measurements.

3. Measurement methods and loss calculation

The measurement methods for each part of the system and how the losses are calculated are described. The power commands issued to the vehicle system (via the VSL) in order to solicit the vehicle according to the expected theoretical losses and to the charging-discharging cycles are included.

3.1. Building electrical components

In this section, the measurement methods of the building electrical components are described.

3.1.1. System analysis

From a theoretical perspective, the losses occurring within the EVSE and the breakers can be divided into two kinds: the stand-by losses, which are constant independently of current flow, and the Joule effect losses or I^2R losses proportional to the square of the current flowing through the components in question.

The losses occurring in the transformer are also twofold. First, according to [23], there are the *no*-load losses which are fixed values and are unrelated to the load. These losses include *hysteresis losses, eddy current losses, dielectric losses, and thermal losses due to no-load current*. Second are load losses dependent upon the loading on the transformer. According to [23], the load losses include the *copper losses* that are proportional to the square of the current flowing in the transformer.

The objective is to measure losses during both charging and discharging, as well as for a range of current values. By using the VSL to control the AC power flow at the PEU, charging and discharging periods at low (10 A), medium (30 A) and high steady currents (42 A) are set.

3.1.2. Loss calculation

For each component, each current value, and each mode (charging or discharging), percentage losses were computed according to equation (1) [24]:

$$l = 100 \times \frac{P_{in} - P_{out}}{P_{in}} \tag{1}$$

with l the power losses in percentage, and P_{in} and P_{out} respectively the instantaneous power *going in* and *going out of* the component in question with respect to the current flow direction. The above formula derives from the efficiency definition, which is the power output divided by the power input [24]. Note that as charging and discharging periods with *steady* current rates were enforced, the instantaneous power values are steady for the entire system and for each experiment.

3.2. EV components

In this section, the measurement methods of the EV components are described.

3.2.1. System analysis

Battery losses are due to several factors, among which are undesired electrochemical reactions within a battery, bad battery condition management by a battery management system (BMS), and cell warming due to internal resistance [25]. Accounting for such losses from a theoretical point of view is beyond the scope of this paper. Rather, the overall battery losses that are dependent upon macro-factors are assessed. Therefore, the battery losses as a function of the battery SOC and current were measured. Previous studies tested different SOCs at constant current [26], or found current to minimize losses [27]. These previous studies supported this study's decision to vary SOC and current as parameters affecting battery internal losses.

Regarding other EV components, the PEU losses consist of two parts: stand-by losses inherent in the electronics, and Joule effect losses proportional to the square current [28]. Therefore the current rate is one significant parameter for the PEU power loss behavior.

The experimental process developed by the authors is based on the parameters SOC and current rate, and on the concept of counting coulombs (Amp-seconds). The losses occurring in the battery and in the PEU are simultaneously assessed during the experiments. Each experiment consists of neutral amp-second round-trips applied at the DC bus level, or in other words, same number of coulombs are charged to and discharged from the battery. Although the same number of coulombs are entering and leaving the battery, the energy into and out of the battery are not the same due to the discharge voltage being lower than the charge voltage at the battery terminals. This method is necessary because

Table 1
Accuracy of measuring devices in % of the reading value.

	AC Meters	DC Meter
Voltage	±0.5	±0.2
Current	±0.5	±0.2
Active Power	±1.5 (±0.5 for EKM)	±0.5

there is no practical way to measure losses inside the battery. For the PEU, losses are more directly measured by voltage and current (and thus power) measured on the input and the output sides.

In order to balance coulombs in battery round-trips, the amp-second flow on the DC bus was monitored in real time by using the DC meter. When the desired number of amp-seconds was reached, a python script automatically changed the charging AC current to discharging and vice versa by communicating with the VSL (see 2.2).

In order to obtain losses as a function of the SOC, the SOC should not change substantially within an experiment. The SOC deviation remained less than 1%.

These round-trips were performed for various steady AC current values and battery SOC values. Measurements were conducted for different combinations of current rates in the range of 10–70Amps and SOCs in the range of 20–80%. The selected values of current and SOC are typical during actual charging and discharging operations when performing grid services.

During each experiment, voltage, current and power were recorded from the DC meter (DC bus just after the battery), and the AC meter (just after the PEU).

Additional information on the experimental procedure can be found in Appendix A.

Since temperature can affect battery performance [26] and the measurement site was inside a building but not space conditioned, the battery temperature was recorded for each experiment and measurements were made only on days with moderate indoor temperatures. Recorded temperatures were within the range of 77–83°F, (25–28°C), well within the mid-range of specified operating temperatures for the vehicle systems.

3.2.2. Loss calculation

Let's consider an experiment consisting of a set of round-trips performed at fixed SOC and AC current values. Let I_{DC} be the battery current, and t_i, t_{c_i} and t_{d_i}, respectively be the starting time, charging duration and discharging duration of the ith round-trip. Then, considering N number of round-trips, the battery capacities are calculated as follows [29]:

$$C_{in} = \sum_{i=1}^{N} \int_{t_i}^{t_i+t_{c_i}} I_{DC}(t)\mathrm{d}t \tag{2}$$

$$C_{out} = \sum_{i=1}^{N} \int_{t_i+t_{c_i}}^{t_i+t_{c_i}+t_{d_i}} I_{DC}(t)\mathrm{d}t \tag{3}$$

with C_{in} and C_{out} respectively representing the total capacity injected in and withdrawn from the battery.

By controlling the charging and discharging durations, the overall net Amp-hour flow is kept null, that is:

$$C_{in} - C_{out} \approx 0 \tag{4}$$

In order to guarantee equation (4), a method to estimate the accuracy of each experiment was developed. The accuracy of these experiments depends on the authors' diligently keeping the measured capacity (amp-seconds) on the DC bus very close to net zero. Despite the automatic control used, there were occasional errors. These errors were constantly measured. The selected test results have errors below 0.1%. The procedure for the accuracy estimation includes the calculation of the total capacity injected in and withdrawn from the battery. Then, for all the experiments the following ratio is calculated:

$$\frac{C_{in} - C_{out}}{C_{in} + C_{out}} \tag{5}$$

with C_{in} and C_{out} respectively representing the total capacity injected in and withdrawn from the battery. For each experiment, the above number should be less than 0.1% so as it can be included in the results.

During those cycles, energy flows on the AC and DC lines, allowing us to define the four quantities $E_{AC_{in}}$, $E_{AC_{out}}$, $E_{DC_{in}}$, and $E_{DC_{out}}$, each respectively standing for the cumulative energy flowing from the EVSE to the PEU, from the PEU to the EVSE, from the PEU to the battery and from the battery to the PEU during the N cycles [24]:

$$E_{AC_{in}} = \sum_{i=1}^{N} \int_{t_i}^{t_i+t_c} V_{AC}(t) I_{AC}(t)\mathrm{d}t \tag{6a}$$

$$E_{AC_{out}} = \sum_{i=1}^{N} \int_{t_i+t_c}^{t_i+t_c+t_d} V_{AC}(t) I_{AC}(t)\mathrm{d}t \tag{6b}$$

$$E_{DC_{in}} = \sum_{i=1}^{N} \int_{t_i}^{t_i+t_c} V_{DC}(t) I_{DC}(t)\mathrm{d}t \tag{6c}$$

$$E_{DC_{out}} = \sum_{i=1}^{N} \int_{t_i+t_c}^{t_i+t_c+t_d} V_{DC}(t) I_{DC}(t)\mathrm{d}t \tag{6d}$$

with V_{AC} and I_{AC} the voltage and current on the AC line respectively, and V_{DC} and I_{DC} the voltage and the current on the DC line respectively.

The percentage energy losses occurring in the battery (l_{bat}), in the PEU while charging (l_{PEU_c}), in the PEU while discharging (l_{PEU_d}) and the EV component overall losses (l_{EV}) are calculated as follows [24]:

$$l_{bat} = \frac{E_{DC_{in}} - E_{DC_{out}}}{E_{DC_{in}}} \tag{7a}$$

$$l_{PEU_c} = \frac{E_{AC_{in}} - E_{DC_{in}}}{E_{AC_{in}}} \tag{7b}$$

$$l_{PEU_d} = \frac{E_{DC_{out}} - E_{AC_{out}}}{E_{DC_{out}}} \tag{7c}$$

$$l_{EV} = \frac{E_{AC_{in}} - E_{AC_{out}}}{E_{AC_{in}}} \tag{7d}$$

3.3. Method limitations

The aforementioned method has some limitations described here.

- One building electric system and two vehicles are tested in great detail, so variance among systems is not captured. In fact, one vehicle's measurements are reported only briefly because it appeared to be anomalously inefficient (described later). Nevertheless, as a first and unique study, the results are

insightful and identify component systems that merit further measurements.
- All the system components are viewed in terms of their input and output. Their internal behavior is out of the scope of this study.
- Since the measurements are charging and discharging only a single vehicle on a transformer designed to charge 15 vehicles, the building transformer operates far below its rated power.
- Given that this is an in situ field measurement campaign over several months, with mobile instruments, not a controlled environment, there are inaccuracies from both uncontrolled variables and sensor drift.

4. Experimental results

The results in measured losses are presented first for building electrical components, then for EV components.

4.1. Building electrical components

The building components were measured at the UD GIV laboratory. Experimental results for building components are presented in Table 2 for charging and discharging modes. Losses are shown both in Watt values as well as in percentages of the DC power according to equation (1). Based on the AC meter accuracy there is an uncertainty of ±1.5% in the measurements [19].

EVSE losses are very low (between 0.1 and 1.48%). They tend to increase when the current increases, thus they are probably mainly resistive losses.

Breaker losses are rather low (between 0.0 and 2.8%), and are presumably resistive losses in breakers and contacts that are expected to increase with current. They generally appear higher as current rises. However, the losses are not proportional to the current and are not even monotonic, and they are also not symmetrical while charging and discharging. This suggests some experimental variability or measurement errors, especially at those low values.

The losses occurring in the transformer are the highest of the building components, for both charging and discharging modes (10.2% and 14.6% for $I_{AC} = 10A$, respectively), because the transformer is operating far below its rated power (300 kVA versus 12 kW), as confirmed by the fact that relative losses decrease when the current increases. Thus, the losses are mostly *iron losses* (see section 3.1.1), and these stand-by losses are high as a fraction of the experimental power flows. According to transformer efficiency curve [30], in more typical use with more of the 15 EVs operating, the fractional losses would be significantly lower. For that reason, when generalizing about the points of greatest losses in the entire building-and-EV system, the atypically high percentage losses for the 300 kVA transformer charging a single vehicle at 10 or 30 amperes are not considered.

Although there is some measurement error in these field measurements, some general observations arise: losses in building electrical components are very low; the only building element with losses reaching almost 15% is the transformer when loaded far below its rated power (≈12% loss at 1% of rated or 5% loss at 3% of rated.) Otherwise, the primary locations for efficiency improvements appear to be on-board the vehicle.

Table 2
Charging and discharging losses of building components.

Component	AC current (A)	Absolute losses (W) (±1.50%)		Percentage losses (%)	
		Charging	Discharging	Charging	Discharging
EVSE	10	2.00	27.00	0.10	1.42
	30	22.50	83.50	0.32	1.48
	42	30.00	100.50	0.29	1.39
Breakers	10	0.00	66.90	0.00	2.80
	30	109.80	201.30	1.50	2.80
	42	132.80	60.50	1.30	0.60
Transformer	10	274.00	339.90	10.20	14.60
	30	602.10	677.80	7.60	9.70
	42	352.00	666.00	3.33	6.65

4.2. EV components

In this section, the results of the measured losses in the EV components, including the battery and the PEU are presented.

4.2.1. Battery losses

Round-trip losses inside the battery, computed according to equation (7a), are presented in Table 3.

Battery losses increase significantly with the current. Regarding losses dependency on SOC values, no particular trend is emerging. The round-trip percentage battery losses are between 1.15% and 7.87%, which is coherent with the literature [31]. Additionally, laboratory experiments on a battery module up to 50Amps DC current were conducted in order to check the consistency of the field measurements. As shown in Appendix B, under this more controlled measurement environment, the same trends for the battery losses are observed.

4.2.2. PEU losses

PEU losses can be measured and computed separately when charging and discharging. The loss, computed according to equations (7b) and (7c), are presented in Tables 4 and 5 respectively. The losses in the PEU were measured between 0.88% and 16.53% for charging, and 8.28% and 21.80% for discharging, reaching the highest losses of any EV or building components. Generally, with some exceptions, percentage losses are higher at lower current, more consistently for charging than discharging. Some very high losses are found at low SOC (again, with exceptions). For charging, generally the higher efficiencies are achieved at higher SOC and higher current. For discharging, no monotonic trend is apparent, with 17.5%–21.8% losses under all conditions (the upper-left 8.28% discharging loss is anomalous, suggesting a measurement error). Discharging loss is always higher than charging loss (with the upper left again anomalous). Also, PEU losses are greater than round-

Table 3
Round-trip loss within battery (%) as a function of the battery state-of-charge (SOC) and the AC current.

		SOC			
		20%	40%	60%	80%
AC Current	10 A	1.37	1.15	1.28	1.34
	30 A	2.74	3.26	2.50	2.65
	50 A	5.04	4.39	4.33	3.85
	70 A	6.39	7.87	6.27	5.27

Table 4
PEU Charging Losses (%) as a function of battery SOC and AC current.

		SOC			
		20%	40%	60%	80%
AC Current	10 A	16.53	2.10	5.30	1.19
	30 A	5.91	7.68	5.73	7.82
	50 A	4.12	5.43	4.64	4.77
	70 A	1.96	2.36	0.88	2.33

Table 5
PEU Discharging Losses (%) as a function of SOC and AC current.

		SOC			
		20%	40%	60%	80%
AC Current	10 A	8.28	17.64	21.80	18.94
	30 A	20.71	19.50	20.85	19.76
	50 A	18.03	19.01	17.92	18.00
	70 A	18.36	17.77	17.70	17.55

trip battery losses under all conditions except charging at the highest currents; PEU losses are also higher than all building components (excepting as noted the low-load whole-building transformer).

A second MiniE was also measured, with the primary difference being that the PEU losses were much higher, especially at low SOC and low current. This vehicle was so far away from manufacturer specifications that its results are not extensively tabulated here. Nevertheless, this second vehicle is a caution that power electronics can perform out of specifications. For example, at 50Amps and 80% SOC, charging losses were 11% and discharging 18%, slightly high. But at 10 Amperes and 20% SOC, charging losses were a staggering 74% and discharging losses were 51%. These extreme inefficiencies were not apparent to technical staff working on the vehicle until the measurement campaign reported here, with external instruments and varying over the full range of conditions of SOC and current.

4.2.3. EV losses in GIV operation

Round-trip losses for all EV components, measured as a whole system according to equation (7d), are shown in Table 6. These losses include PEU and battery losses, with the larger PEU losses having a greater effect on the overall system losses. Round-trip losses of all EV components are fairly uniform because the totals are dominated by the largest loss, PEU discharging, which is also fairly uniform. The individual losses from Tables 3–5 can be checked against the whole system losses by taking the product of each component's efficiency. The comparison shows that the 10Amp and 70Amp values are very close, that is, the whole system measurements validate the measured individual components losses within approximately 0.0% to 3.5%. However, the 30Amp and 50Amp values are lower in the whole system measurements of Table 7, with the product of components around 26% and the whole system measurement about 18%. From the nonlinearity of losses at different ampere values, it is concluded that the whole system measurements at 30 and 50Amp are low. Other than Fig. 2, the individual component values are therefore used for subsequent calculations.

The general trends and factors of EV losses are more easily understandable by plotting the losses in electrical units (kW) rather than percent. Fig. 2 shows the round-trip EV system losses in kW as a function of AC input power, also in kW. The intercept of losses is about 0.6 kW, and as the input power increases, the losses increase as well. Two separate interpolation curves for high SOC (> 50%) and low SOC (< 50%) are plotted. The interpolation functions are second-order polynomial. The two SOC curves are more easily distinguished at high AC power applied (> than 8 kW, the right side of the graph), with higher loss for low SOC than for high SOC. Also, for higher AC power applied, absolute losses are seen to be higher, even though, as seen previously, the percentage loss is higher at low power.

Table 6
Round-trip losses of all EV components as a function of the SOC and the AC current (in %).

		SOC			
		20%	40%	60%	80%
AC Current	10 A	24.49	20.30	26.89	19.08
	30 A	18.33	16.15	18.41	15.77
	50 A	18.96	18.36	17.83	17.40
	70 A	22.08	22.45	22.19	20.07

There is a diversity of charger electronics technologies with different characteristics [16]. The vehicle tested uses a polyphase pulse width modulated inverter and boost switching regulator [32]. With the diversity in charger topologies, one would expect some differences in the curve of Fig. 2, depending on the topology. Nevertheless, theoretically it would be reasonable to expect that most or all charger topologies would exhibit the same pattern of a constant standby loss plus an additional variable loss that increases with throughput power.

4.2.4. Summary: total system losses, building plus EV

Percentage losses for charging and discharging for all building plus EV components are in Table 7 for 10Amps and 40Amps.[3] The EV values are average for all SOCs. Because the battery losses cannot be measured separately for charge and discharge, each is assumed to be half the total losses. The battery charging and discharging losses are assumed equal for 10Amps [33]. For high currents, the discharging losses start increasing until reaching approximately 10%, because the internal resistance becomes higher [33]. Here, it is assumed approximately 6% higher discharge loss for 40Amps.

Combining all parts of the system, the general conclusions from Table 7 are:

a) the PEU losses are highest of all components in either EV or building, (disregarding the transformer behavior when underrated)
b) the charging losses are less than the discharging losses, and
c) the percentage losses are less at mid and high current charging.

5. Discussion of findings on efficiency and losses

Overall, compared with the magnitude of losses in the building electrical system, and compared with the losses in the battery itself, the PEU losses dominate all the system losses. Further, because PEU efficiency varies at different operating parameters, in order to achieve maximum efficiency, charging and discharging are most efficient at the different currents shown in Tables 4 and 5.

There is little discussion of EV charging efficiency issues in the literature, even less if considering bidirectional charging. Typically, efficiency is measured under design conditions, that is, using voltages V_{in} and V_{out} that are at design conditions, whereas battery voltage at low SOC may be quite different from those. Specifications typically also assume charging current at the mid or upper range of design specifications. Manufacturer efficiency curves may show drop-off in efficiency occurring at low currents, but do not graph for differences in voltage. For example, the manufacturer's specification sheet for the charger tested here [34] shows $208V_{AC}$ charging at the lowest efficiency of 80% at 1 kW (5Amps), moving up to 90% at 2.5 kW (12Amps), and reaching 95% efficiency above 6 kW (30Amps). Charging at $120V_{AC}$ and 2.5 A was only 50% efficient, at 120 V and 8 A only 80% efficient – indirectly acknowledging that AC voltage (as well as current) have a large effect on efficiency. Upon comparison of the manufacturer 2-D efficiency curve (power vs. efficiency) with the 3-D curve (including SOC), it is shown that the

[3] The EVSE, breaker and transformer values are for 42Amps.

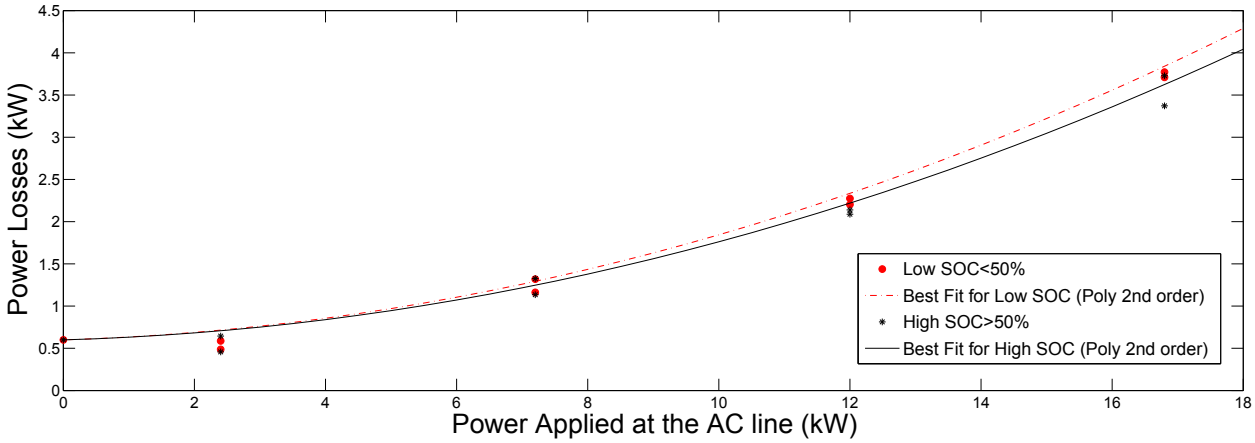

Fig. 2. Round-trip EV Losses against AC power applied, both expressed in absolute kW.

Table 7
Total GIV system percentage losses: building and EV components.

Component	AC current (A)	Percentage losses (%)	
		Charging	Discharging
EV Battery	10	0.64	0.64
	40	1.69	1.91
EV PEU	10	6.28	16.67
	40	5.77	19.23
EVSE	10	0.10	1.42
	≈40	0.29	1.39
Breakers	10	0.00	2.80
	≈40	1.30	0.60
Transformer	10	10.20	14.60
	≈40	3.33	6.65
Total	10	17.22	36.13
	40	12.38	29.78

closest to the specification sheet would be to test with the battery over 70% SOC and charge current at least 30Amps (6 kW). Thus, the main differences between the measured values and the data sheet values probably come from the manufacturer-undocumented SOC of the battery and the operating conditions of the PEU (input voltage and currents, ambient temperature, etc.). A quick perusal of other charger specification sheets or research reports leads credence to these findings.

Few academic articles present complete test data on EV charging efficiency, for example, they may include tests only near design conditions (e.g. Ref. [28] with EVSE efficiency), and in charging mode only [27]. The [35] shows EVSE efficiency curves from simulations and under limited conditions. Similarly to the results presented here, considering the EVSE only, the simulations showed very low losses, under 3% in all cases tested (3.3 kW and 33.5 kW rates) [35]. One practical guide (non-research) noted that charging efficiency varied greatly with battery SOC [36]; but in that guide the battery type and charger technologies were older and very different from this study. The only two research articles that measured effects of both SOC and current (charging only) were [27,36], finding significant effects on efficiency. None of those prior studies measured a complete system, including building supply, EVSE, EV power electronics and battery, nor did any loss measurement for two way power flow. However, by taking partial results from these other studies, some of the general trends observed here are validated.

These high percentage losses are not surprising in charging equipment that must be designed to operate over a wide range of currents, and voltages, as EV chargers do over a range of charging stations. This makes EV chargers more difficult to optimize over their full range of conditions. (Other devices, such as laptop computers and cell phones, charge at varying and lower rates only as the battery reaches full.) EVs when providing grid services may charge or discharge at many different rates. As the data illustrate, at some of those rates the system may be suboptimal.

For discussion, an EV drivers' view of these efficiency issues is considered. These losses are invisible to the user or driver, either in charging mode or when providing grid services. Thus there is no direct feedback that the user should keep within the more efficient regions of the space as shown in Tables 3–5. Further exacerbating the problem, low-power home charging is often recommended to EV buyers, as it requires minimal electrical work.

Based on these empirical findings, the authors have developed suggestions for overnight charging and algorithms for the most efficient operation of grid services. In the next section, the effects of these low efficiencies on simple charging and their influence on developing specifications of EVSE equipment are discussed. Then, how the efficiencies should affect grid-integrated vehicle dispatch algorithms for the provision of grid services is explored.

6. Engineering for non-linear loss functions

The results presented in section 4 show that losses are highly localized whether in EV charging or in GIV charging and discharging. Loss in the battery and in PEU depends on both current and battery SOC. Quantitatively, the PEU is responsible for the largest amount of loss, which varies widely based on the two aforementioned factors.

In this section, engineering solutions for reducing losses are explored. First, strategies for setting Ampere specifications for simple charging are discussed. The second, and larger, part of this section compares two dispatch algorithms for GIV. The first algorithm does not take the results from this article into account whereas the second one is based on the experimental measurements and minimizes losses.

6.1. Specification of EVSE amperes for simple charging

Assume that the site engineering specifies the electrical connections at a location for a home, or a business charging station where the vehicle will be parked overnight and weekends. Typically the time parked and the kW power versus needed kWh charge in the morning are considered. Therefore, if a typical daily commute or commercial route requires 15 kWh, and the car will always be

Table 8
Three options of EV charging: charging rates 8Amps at 120 V, 10Amps and 70Amps at 240 V.

Charging rate (Amps)	EVSE voltage (V)	EV losses (%)	Required energy (kWh)	Yearly amount ($/year)
8	120	20.00	4114	531
10	240	6.92	3665	473
70	240	4.78	3592	463

parked at least 10 h, one might consider that 1.5 kW would be sufficient. Unless higher power is needed for contingencies (e.g. a fast recharge at the home base between trips), this might be specified as 230 V or 240 V at 8Amps, or, in the U.S., 120 V at 12Amps.

A vehicle with a small charger may be optimized at a low charging rate, today that would typically be 7 kW for a battery vehicle and 3 kW for a plug-in hybrid. But the "minimum needed" specification mentioned above would be running a 7 kW charger at 1/4 to 1/8 of it's rated power, or an 18 kW charger, like that used here at 1/12 of rated power. If the findings of reduced efficiency at low power were applied to the hypothetical charger being considered here a specification of 1.5 kW may lead to overnight charging at a low efficiency. Such efficiency consideration is not generally considered in specification of EVSE amperes or kW capacity.

Does it make economical sense to use an EVSE that lowers the efficiency? Using the specific efficiency values of the charger investigated here, the costs of two different residential EVSEs are calculated.

To evaluate this question, three options are compared. It is common for EVs to come with a portable cable including a charger in-line at 120 V (US) or 230 V (EU and Asia). At 120 V and 8Amps this provides about 1 kW. Many EV buyers use this as their primary charging device, although as cited above, efficiency at 1 kW is only 80%. This is compared with the measurements for two installed chargers. From Table 3, by averaging for all SOCs, the 10Amps and 70Amps roundtrip battery losses are 1.29% and 6.45% respectively. According to [33], for low currents charging and discharging battery losses are equal, while for higher currents, the discharging losses are approximately 10% more compared to the charging losses. Therefore, the battery percentage charging losses for 10Amps are 0.64%, and for 70Amps are 2.9%. The PEU percentage losses (see Table 4) are 6.28% for 10Amps and 1.88% for 70Amps. The percentage losses of battery and PEU for charging mode are summed. Assuming one year of charging with an average of 12,000 miles driven and 3.5 mi/kWh, the energy needed would be 3,428 kWh per year. For each entry in Table 8, the needed 3,428 kWh is increased to account for losses. With US average residential price at $0.129 per kWh [37], two options are explored presented in Table 8:

The supplied 8Amps, 120 V charger is free, but adds approximately $60 to the annual cost of recharging. A 10 Amp, 240 V permanently-installed EVSE might cost $600 installed, while a still higher power (70 Amp) EVSE installation might increase the cost by $500.[4] Incremental cost from the supplied cable-charger to an installed 240 V EVSE would pay off in ten years, but savings from moving to much higher Amperes would save only $10 per year. Therefore, efficiency alone could justify the step from first to second level, not the second step to highest power. The example picks one PEU and uses this article's measurements to illustrate the calculation, concluding that higher power sometimes may be cost-effective solely due to efficiency. For other EVs, efficiencies at the differing power levels would have to be measured, and cost-effectiveness separately calculated. (Higher power may have other benefits, such as driver flexibility to recharge during a stop between trips, higher revenue from grid services, etc.)

[4] EVSE prices usually include the charging station itself, its installation by a certified technician, possible upgrading of household electrical circuits, and so on. Therefore, cost depends a lot on the existing installations, the location etc. For instance, the company Sodetrel (France) offers the installation of a wall-mounted Schneider Electric for 1086€, i.e. $1231 [38].

6.2. Dispatch algorithms for grid services

In this section, after describing the simulation scenario for a GIV system, two dispatch algorithms are compared (the equal and the high efficiency dispatch algorithm).

6.2.1. Simulation scenario

The second engineering problem is dispatch of a group of EVs for grid services. Ten EVs ($N_{EV} = 10$) permanently plugged-in at 12 kW charging stations and available for grid services are considered. These vehicles participate in the frequency regulation market as organized by PJM, a US TSO, and are controlled by a central aggregator that receives a signal from PJM on a 2-s basis. This signal value, ranging between −1 and 1, is then converted by the aggregator into a power setpoint for each EV in the vehicle fleet. The aggregator is responsible for dispatching this power among the vehicles, by means of a dispatch algorithm. Two different dispatch algorithms are compared here for 4 time slots of 8 hours each. This simulation duration corresponds to a typical plug-in duration at home for the night or at a workplace during the day.

In both algorithms, this article's experimental results are used to assess the losses of each EV at each moment, depending on the requested current and on the battery SOC. In order to build a continuous loss behavior as a function of current and SOC (since the data measured are discrete), linear interpolation was used based on the values provided in Tables 3–5. As a result, a surface that represents the impact of current rate and SOC on the losses was developed. Fig. 3 provides the result of the linear interpolation for the total round-trip losses. The simulation is based only on the battery and charger losses because only those are non-linear (except the large under-used transformer, which is rather unique to this building configuration). The initial battery SOCs are evenly distributed in the 20%–90% interval for all simulations in both algorithms.

6.2.2. Equal dispatch algorithm

The equal dispatch algorithm operates as follows. First, the aggregator identifies all EVs available for regulation, that is, the EVs that have a SOC more than 20% if discharging power is requested or less than 90% if charging power is requested. It then simply divides the requested power equally among the available EVs, with respect to the maximum charging power (here assumed to be 12 kW). The average energy losses over the 8 h for the ten vehicles are of 32.27 kWh.

6.3. High efficiency dispatch algorithm

The high efficiency dispatch algorithm solves the following optimization problem for each time stamp i:

$$\min_{P} \sum_{k=1}^{N_{EV}} \left| Losses_i^k \right| \tag{8}$$

Under constraints:

$$\forall k \in [\![1; N_{EV}]\!], -12kW < P_i^k < 12kW \tag{9a}$$

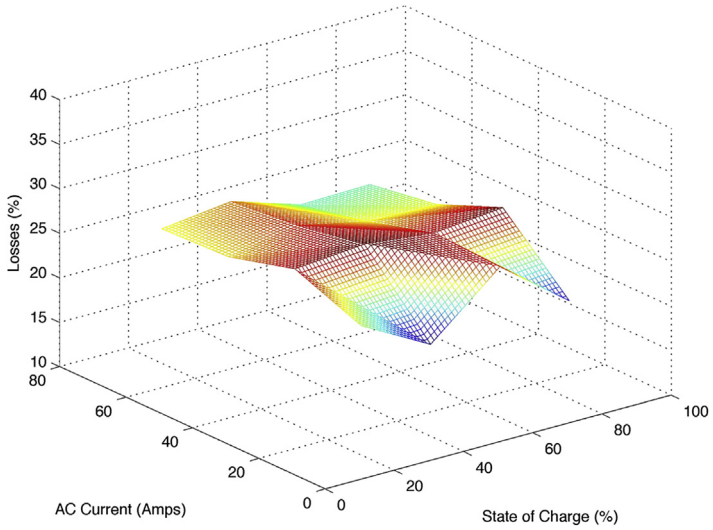

Fig. 3. Interpolation of round-trip losses (PEU and Battery).

$$\forall k \in [\![1; N_{EV}]\!], 20 < SOC_i^k < 90 \tag{9b}$$

$$\sum_{k=1}^{N_{EV}} P_i^k = P_{req_i} \tag{9c}$$

$$\forall k \in [\![1; N_{EV}]\!], SOC_i^k = SOC_{i-1}^k + P_i^k * \Delta t \tag{9d}$$

with P_i^k and SOC_i^k respectively representing the instantaneous power and SOC of vehicle k at time i, P_{req_i} the power requested by PJM at time i, Δt the simulation sample time (here, 2 s) and $Losses_i^k$ the power losses occurring in vehicle k at time i. Constraints (9a) and (9b) ensures that individual EV power and SOC do not exceed their limitations, constraint (9c) stands for the entire requested power provided by the fleet, and constraint (9d) stands for the system dynamics.

The simulation results in average losses of 29.53 kWh for the high efficiency algorithm, approximately 8.5% less losses than the equal dispatch algorithm. For the 4 time slots tested, the high efficiency dispatch algorithm improves the losses from 6.96% to 9.66%.

Comparing the two economically, to provide one MW of regulation for one day would require 10× the power of the example above, over 3× the time. One MW over 24 h at a recent PJM $30/MW-h market price would generate $720. At an energy cost of $0.129 per kWh [37], the equal dispatch algorithm would cost 968 kWh in makeup energy or $124.9. The efficiency algorithm would cost 886 kWh, replaced at a cost of $114.3.

7. Conclusions

Experimental measurements were carried out of the power losses occurring in all the components of a whole GIV system, including the building circuits and the EV. Each subsystem's power loss was measured separately. For the building components a range of current values was tested. For the EV components different combinations of current and SOC were tested. Losses vary depending on the current and on the EV SOC.

Based on these experimental results, the authors quantitatively analyzed design choices to operationally reduce losses, either by sizing of EVSEs (only charging), or by dispatching algorithms of grid service providers (charging and discharging).

First, consideration of efficiency in sizing a charging station is recommended. Charging at the lowest rates may require lower capital cost but can incur higher energy cost. Picking optimum charger power requires calculation of payback for differing devices.

Additionally, analyzing the efficiency of dispatching of grid services, two dispatch algorithms for the provision of grid services were compared quantitatively. Results show an 8.5% decrease in losses when the efficiency curve from experimental measurements is taken into account in the algorithm.

Both experimental results and charging algorithms proposed are based on one specific EV charging system and the specific efficiency curve is particular to that EV system. Therefore, the precise efficiency values here will differ among EVs and electrical circuits. It is common, however, for both AC to DC (charging) and DC to AC (discharging) topologies to exhibit highest efficiency at the top region of their rated power – and conversely, to exhibit low efficiencies at power levels less than half of their rated power. Based on both general principles and on the cursory comparison of other charger specifications, the general findings should hold over many or most EVs.

Acknowledgment

The empirical work reported in this paper was funded by a joint venture between an NRG Energy EV group and the University of Delaware; the NRG EV group is now a separate spinoff called EVgo Services, LLC. Part of the research was also financially supported by the U.S. Department of Energy via the National Renewable Energy Laboratory (NREL), as "Open V2X at ESIF", Subcontract No. NCS-5-42326-05, which also paid for open access. The authors thank the NREL staff, including Andrew Meintz and Mike Simpson from the Energy Systems Integration Facility (ESIF) for support of some of the vehicle efficiency measurements reported here. Also, the authors are grateful to Matthias Kluck and AutoPort, Inc for the advice and assistance with the MiniE and to BMW AG, including Peter Krams and Xaver Pfab for making the BMW MiniE's available for this project. Yushan Yan provided battery testing equipment, and David Mroz, Brandon Budenz, Annette Brocks and Tianne L. Lassiter assisted in the experiments and measurements. Sachin Kamboj, Stijn Vandael and Rodney McGee provided essential software and hardware engineering support for the measurement campaign, and Dr. Daniel Lees proofread the manuscript. Yosef Shirazi and Hikari Nakano provided valuable checking of qualitative results.

Paul Codani benefits from the support of the Chair "PSA Peugeot Citroen Automobile: Hybrid technologies and Economy of Electromobility", called the Armand Peugeot Chair led by Ecole CentraleSupelec and ESSEC and sponsored by Peugeot Citroen Automobile.

Appendix A. Additional information on the experimental procedure for EV component losses measurements

In this section, additional information on the experimental procedure is provided via example figures. Fig. A.4 displays the recordings of one experiment, with the amp-second neutral cycle on Fig. A.4a and the corresponding energy exchanged between the EV and the EVSE on Fig. A.4b. This test was performed for $I_{AC} = 21A$ and $SOC = 60\%$.

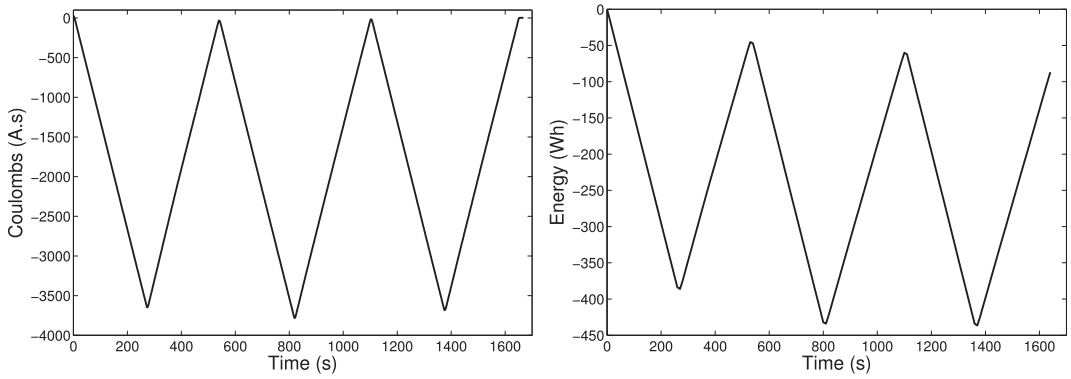

(a) Coulomb flow on the DC bus (b) Energy flow on the AC line

Fig. A.4. Results of an efficiency test performed at AC 21Amps, with SOC = 60%.

Appendix B. Lab battery measurements: checking for consistency with field results

Regarding the battery measurements, the same experiments were conducted on a battery module in a laboratory in order to check the consistency of the field experiments.

The battery module $LiPF_6$ consists of 53 cells in parallel and 2 in series. The Arbin Instruments BT-2000 was used to implement DC current command, while also recording DC voltage, current, energy and power. The same cycles as described in Appendix A were applied, for various DC current and SOC values. The loss calculation method was therefore same as the one detailed in 3.2.2. Results are provided in Fig. B.5.

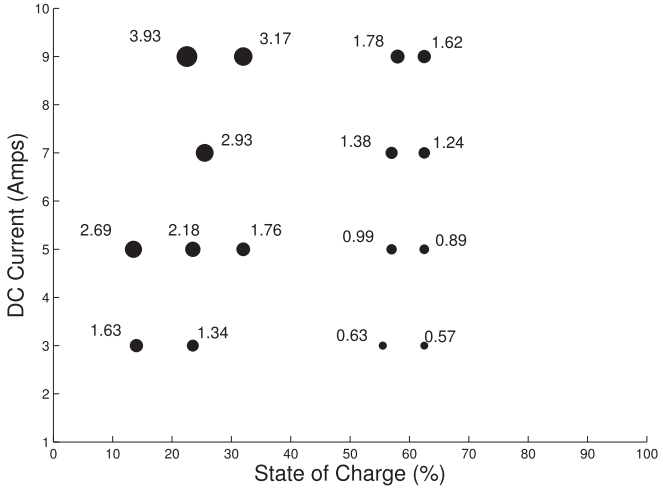

Fig. B.5. Battery module losses as a function of the SOC and the DC current (in %). Experiments were conducted in the laboratory. No PEV or AC electric components are included.

The lab battery test results show similar trends to the field battery tests: losses increase with the current, thus strengthening the field battery loss results.

Appendix C. Measuring devices

Appendix C.1. DM-II PLUS Power Quality Analyzer calibration

The *DM-II PLUS Power Quality Analyzer* AC meter, manufactured by Amprobe company, was used for AC measurements. The clamp and the meter were calibrated by using the Power Energy Logger PEL 103 by AEMC Instruments [39]. This device was new and already calibrated by the company.

Appendix C.2. AcuDC 243-C DC meter calibration

The *AcuDC 243-C DC meter*, manufactured by AccuEnergy company, was used for DC measurements. The probe used along with the DC meter is the CYHCS-WLY-300A-14. The rated input current of this probe is 250 A, while the measurements are expected to be in the range 0–30 A on the DC bus. Therefore, the DC probe and the meter were calibrated for low current values. The probe errors ε assessed at low currents, are defined by equation (C.1):

$$\tilde{I}_{DC} = I_{DC} + \varepsilon_{I_{DC}} \tag{C.1}$$

with $\tilde{I}_{DC}$ the measured current and I_{DC} the actual one. A very precise DC current source, Keithley Source Meter 2600, was used. The values measured by the couple probe/meter for several current values were recorded from 5Amps to 30Amps. In the end, the error parameters m and σ for each current value were evaluated such that:

$$\varepsilon_{I_{DC}} \sim \mathcal{N}\left(m_{I_{DC}}, \sigma^2_{I_{DC}}\right) \tag{C.2}$$

with $m_{I_{DC}}$ and $\sigma_{I_{DC}}$ respectively the mean and standard-deviation of the errors. It was observed that the standard deviations were rather low and steady. On the contrary, mean errors can reach up to 0.7Amps for 30Amps, which triggers a 2.3% error. Matlab curve

fitting tool was used to compute the entire curve of mean errors as a function of the DC current measured (Fig. C.6).

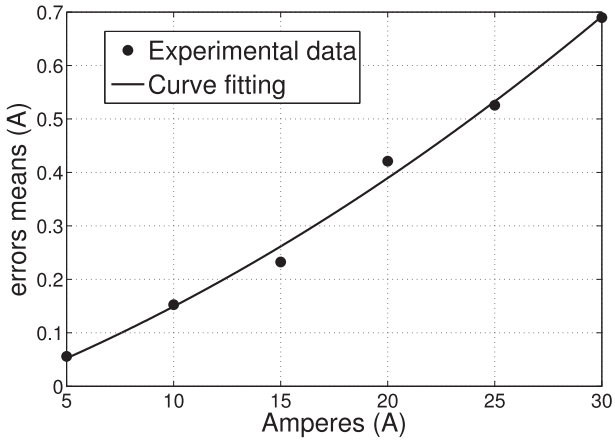

Fig. C.6. Interpolation function for mean errors from the DC meters as a function of the DC measured current.

By using the interpolation function and the real-time communication ability of the AcuDC meter, the probe measures were corrected in real time in order to monitor the Coulomb cycles properly.

Appendix D. Total Harmonic Distortion (THD)

The Total Harmonic Distortion (THD) was measured, but detail on THD is out of the scope of this paper. Briefly, the THD for low and high currents, at lower and higher states of charge were measured using the PEL 103, so as to understand the components of round-trip losses. Results are presented in Fig. D.7. It is true that at lower currents the THD is higher than at higher currents, and THD is higher at lower SOC, but these differences are still marginal compared to the PEU loss values.

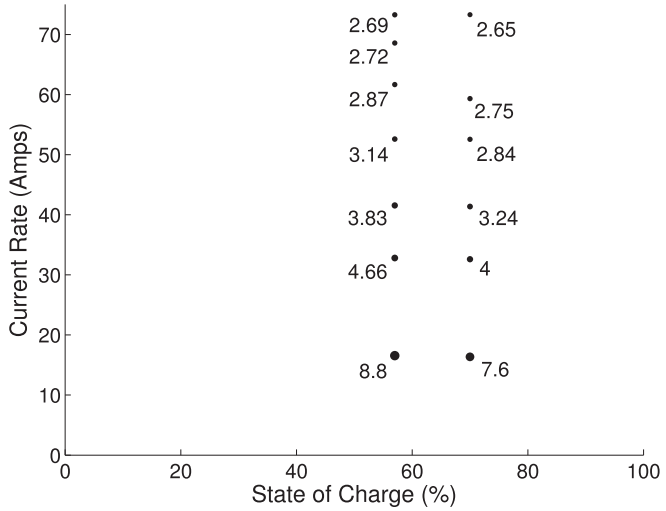

Fig. D.7. Total Harmonic Distortion measurements (in %) during charging.

References

[1] Kempton W, Letendre S. Electric Vehicles as a new power electric utilities source for electric utilities. Transp Res Part D Transp Environ 1997;2(3):157–75. http://dx.doi.org/10.1016/S1361-9209(97)00001-1.

[2] Budischak C, Sewell D, Thomson H, Mach L, Veron DE, Kempton W. Cost-minimized combinations of wind power, solar power and electrochemical storage, powering the grid up to 99.9% of the time. J Power Sources 2013;225:60–74. http://dx.doi.org/10.1016/j.jpowsour.2012.09.054.

[3] Clement-Nyns K, Haesen E, Driesen J. The impact of vehicle-to-grid on the distribution grid. Electr Power Syst Res 2011;81(1):185–92. http://dx.doi.org/10.1016/j.epsr.2010.08.007.

[4] Knezovic K, Marinelli M, Codani P, Perez Y. Distribution grid services and flexibility provision by electric vehicles: a review of options. In: 2015 50th international Universities power engineering conference (UPEC). Staffordshire (UK): IEEE; 2015. p. 1–6. http://dx.doi.org/10.1109/UPEC.2015.7339931. http://ieeexplore.ieee.org/lpdocs/epic03/wrapper.htm?arnumber=7339931.

[5] Kempton W, Udo V, Huber K, Komara K, Letendre S, Baker S, et al. A test of vehicle-to-grid (V2G) for energy storage and frequency regulation in the PJM system. manuscript availble from first author or URL. 2008. http://www.udel.edu/V2G/resources/test-v2g-in-pjm-jan09.pdf.

[6] Sortomme E, El-Sharkawi MA. Optimal scheduling of vehicle-to-grid energy and ancillary services. IEEE Trans Smart Grid 2012;3(1):351–9. http://dx.doi.org/10.1109/TSG.2011.2164099.

[7] Kempton W, Tomić J. Vehicle-to-grid power fundamentals: calculating capacity and net revenue. J Power Sources 2005;144(1):268–79. http://dx.doi.org/10.1016/j.jpowsour.2004.12.025.

[8] Codani P, Petit M, Perez Y. Participation of an Electric Vehicle fleet to primary frequency control in France. Int J Electr Hybrid Veh 2015;7(2):233–49. http://dx.doi.org/10.1504/IJEHV.2015.071639.

[9] Wald ML. Two-way charging, electric cars begin to earn money from the grid. April 26 2013. http://www.nytimes.com/2013/04/26/business/energy-environment/electric-vehicles-begin-to-earn-money-from-the-grid.html?_r=0.

[10] Kamboj S, Kempton W, Decker KS. Deploying power grid-integrated electric vehicles as a multi-agent system. In: 10th int. Conf. on autonomous agents and multiagent systems - innovative applications track (AAMAS) 1 (Aamas); 2011. p. 2–6.

[11] W. Kempton, Electric Vehicle Equipment for Grid-Integrated Vehicles, US Patent Number, 8509976 B2 (2013). Also, Aggregation Server for Grid-Integrated Vehicles, US Patent Number 9,043,038 (2015).

[12] Sortomme E, El-Sharkawi MA. Optimal charging strategies for unidirectional vehicle-to-grid. IEEE Trans Smart Grid 2011;2(1):131–8. http://dx.doi.org/10.1109/TSG.2010.2090910.

[13] Han S, Han S, Sezaki K. Optimal control of the plug-in electric vehicles for V2G frequency regulation using quadratic programming. In: ISGT 2011. IEEE; 2011. p. 1–6. http://dx.doi.org/10.1109/ISGT.2011.5759172.

[14] Vandael S, Holvoet T, Deconinck G, Kamboj S, Kempton W. A comparison of two V2G mechanisms for providing ancillary services at the University of Delaware. In: IEEE international conference on Smart grid communications; 2013.

[15] Fernández I, Calvillo C, Sánchez-Miralles A, Boal J. Capacity fade and aging models for electric batteries and optimal charging strategy for electric vehicles. Energy 2013;60:35–43. http://dx.doi.org/10.1016/j.energy.2013.07.068.

[16] Musavi F, Edington M, Eberle W, Dunford WG. Energy efficiency in plug-in hybrid electric vehicle chargers: evaluation and comparison of front end AC-DC topologies. In: IEEE energy conversion congress and exposition: energy conversion innovation for a clean energy future, ECCE 2011, proceedings; 2011. p. 273–80. http://dx.doi.org/10.1109/ECCE.2011.6063780.

[17] Kim JS, Choe GY, Jung HM, Lee BK, Cho YJ, Han KB. Design and implementation of a high-efficiency on-board battery charger for electric vehicles with frequency control strategy. In: 2010 IEEE vehicle power and propulsion conference, VPPC 2010, no. Ccm; 2010. http://dx.doi.org/10.1109/VPPC.2010.5729042.

[18] Bach Andersen P, Garcia-Valle R, Kempton W. A comparison of electric vehicle integration projects. In: 2012 3rd IEEE PES innovative Smart grid technologies europe (ISGT europe), no. 081216. IEEE; 2012. p. 1–7. http://dx.doi.org/10.1109/ISGTEurope.2012.6465780.

[19] Amprobe Company, Dm-ii plus 1000a power quality analyzer data sheet, http://content.amprobe.com/DataSheets/DM-II%20PLUS%20Power%20Quality%20Recorder.pdf, Last Accessed April 26th, 2016 (2014).

[20] EKM Metering Company. Ekm omnimeter pulse v.4. 2016. http://www.ekmmetering.com/omnimeter-pulse%20PLUS%20Power%20Quality%20Recorder.pdf. Last Accessed Nov. 30th, 2016.

[21] AccuEnergy. AcuDC 240 series DC power and energy meters brochure. 2014. https://www.accuenergy.com/files/acudc/AcuDC-240-DC-Power-Energy-Meter-Brochure.pdf. Last Accessed April 26th, 2016.

[22] ChenYang Technologies, CYHCS-WLY-300A-14 data sheet, www.cy-sensors.com/CYHCS-WLY-300A.pdf, Last Accessed April 26th, 2016 (2014). URL www.cy-sensors.com/CYHCS-WLY-300A.pdf.

[23] Georgilakis PS. Environmental cost of distribution transformer losses. Appl Energy 2011;88(9):3146–55. http://dx.doi.org/10.1016/j.apenergy.2010.12.021.

[24] Erickson RW, Maksimovic D. Fundamentals of power electronics. Springer Science & Business Media; 2007.

[25] Broussely M, Biensan P, Bonhomme F, Blanchard P, Herreyre S, Nechev K, et al. Main aging mechanisms in Li ion batteries. J Power Sources 2005;146(1–2):90–6. http://dx.doi.org/10.1016/j.jpowsour.2005.03.172.

[26] Bloom I, Cole B, Sohn J, Jones S, Polzin E, Battaglia V, et al. An accelerated calendar and cycle life study of Li-ion cells. J Power Sources 2001;101(2):238–47. http://dx.doi.org/10.1016/S0378-7753(01)00783-2.

[27] Barbé D. Optimal current setpoint policy for energy losses minimization during battery charging process. In: European electric vehicle congress (EEVC); 2014. p. 1–11.

[28] Musavi F, Edington M, Eberle W, Dunford WG. Energy efficiency in plug-in hybrid electric vehicle chargers: evaluation and comparison of front end

AC-DC topologies. In: 2011 IEEE energy conversion congress and exposition. IEEE; 2011. p. 273–80. http://dx.doi.org/10.1109/ECCE.2011.6063780.
[29] Ng KS, Moo C-S, Chen Y-P, Hsieh Y-C. Enhanced coulomb counting method for estimating state-of-charge and state-of-health of lithium-ion batteries. Appl energy 2009;86(9):1506–11.
[30] Saadat H. Power system analysis. third ed. PSA Publishing; 2010.
[31] Ehsani M, Gao Y, Gay SE, Emadi A. Energy storages. In: Rashid MH, editor. Modern electric, Hybrid electric, and fuel cell vehicles: fundamentals, theory and design. CRC Press; 2004. p. 299–332. Ch. 10.
[32] A. G. Cocconi, Combined motor drive and battery recharge system, US Patent Number 5341075 (1994).
[33] Krieger EM, Arnold CB. Effects of undercharge and internal loss on the rate dependence of battery charge storage efficiency. J Power Sources 2012;210: 286–91. http://dx.doi.org/10.1016/j.jpowsour.2012.03.029. URL, http://linkinghub.elsevier.com/retrieve/pii/S0378775312006283.
[34] AC Propulsion Inc. AC-150 Gen-2 EV power system integrated drive and charging for electric vehicles. 2008. URL, acpropulsion.com.
[35] Tan KM, Ramachandaramurthy VK, Yong JY. Bidirectional battery charger for electric vehicle. In: 2014 IEEE innovative Smart grid technologies – asia (ISGT ASIA); 2014. p. 406–11. http://dx.doi.org/10.1109/ISGT-Asia.2014.6873826.
[36] Boulden D. Optimizing energy usage. In: Energy and fork lift truck batteries. Mount Kisco, NY: Curtis Instruments; 1980. Ch. 4. URL, http://www.evbatterymonitoring.com/WebHelp/whnjs.htm.
[37] EIA, Energy Information Administration. Electric power monthly, average price of electricity to ultimate customers by end-use sector. 2016. https://www.eia.gov/electricity/monthly/epm_table_grapher.cfm?t=epmt_5_6_a%20PLUS%20Power%20Quality%20Recorder.pdf. Last Accessed Nov. 30th, 2016.
[38] Sodetrel, Electric vehicle supply equipment installation offers, http://www.sodetrel.fr/, Last accessed April 26th 2016.
[39] AEMC Instruments, Pel 103 power and energy loggers, http://www.aemc.com/products/html/moreinfo.asp?id=110604&dbname=products, Last Accessed April 26th 2016.